

10 mL of acetone was stirred for 12 h at 25 °C. The solution was then saturated with NaCl, extracted 5 times with diethyl ether, dried over MgSO₄, and concentrated in vacuo to yield 0.903 g (65%) of 4-hydroxybutanoic acid which was used immediately. The crude acid aldehyde (0.903 g, 8.85 mmol), 5.64 g (17.7 mmol) of Ph₃PCHCOCH₃,²³ and 50 mL of THF were heated at reflux for 24 h under an argon atmosphere. The reaction mixture was quenched to yield 0.612 g (49%) of crude 6-keto-4-heptenoic acid, which was submitted to immediate NaBH₄ reduction (0.64 g, 17.2 mmol) in 20 mL of MeOH for 1 h, giving 0.350 g (56%) of the hydroxy acid (**3**) after column chromatography (1:2, petroleum ether: diethyl ether, SiO₂): ¹H NMR (250 MHz, CDCl₃) 5.62 (m, 2 H, H-4, H-5), 4.28 (app quintet, *J* = 6.2 Hz, H-6), 2.50-2.34 (m, 4 H, H-2, H-3), 1.26 (d, *J* = 6.2 Hz, 3 H, H-7); IR (neat) 3600-3100, 2980, 2940, 1710, 1065, 970; MS *m/e* (relative intensity) 145 (M⁺ + 1, 1.32), 143 (M⁺ + 1 - H₂, 2.17), 127 (M⁺ + 1 - H₂O, 100.00); high resolution mass spectrum (EI) calcd for C₇H₁₀O₂, M⁺ - H₂O 126.0681, found 126.0677.

rel-[5R]-Dihydro-5-(rel-[1S,2R]-2-hydroxy-1-iodopropyl)-2(3H)-furanone (4a) and rel-[5S]-Dihydro-5-(rel-[1R,2R]-2-hydroxy-1-iodopropyl)-2(3H)-furanone (4b). The general procedure for iodolactonization of hydroxyalkenoic acids as reported by Chamberlin et al.^{1a} was followed by using 127 mg (0.882 mmol) of **3** and 672 mg (2.65 mmol) of iodine to yield 186 mg (78%) of crude **4a** and **4b**. **4a**: ¹H NMR (250 MHz, CDCl₃) 4.77 (m, H-5), 4.10 (dd, *J* = 9.5, 1.9 Hz, H-6), 3.44 (m, H-7), 2.60 (m, 3 H), 2.08 (m, 1 H), 1.29 (d, *J* = 6.2 Hz, 3 H, H-8). **4b**: ¹H NMR (250 MHz, CDCl₃) 4.56 (m, H-5), 4.35 (dd, *J* = 9.0, 4.5 Hz, H-6), 3.63 (m, H-7), 2.60 (m, 3 H), 1.88 (m, 1 H), 1.35 (d, *J* = 6.2 Hz, 3 H, H-8) based on integration, the ratio of **4a**:**4b** was 2:1; IR (neat) 3600-3250, 2990, 2940, 1780, 1340, 1175, 1020, 915, 730; mass spectrum, *m/e* (relative intensity) 270 (M⁺, 0.74), 226 (M⁺ - C₂H₄O, 16.34), 127 (I⁺, 2.15), 99 (M⁺ - I - C₂H₄O, 100.00), 85 (C₄H₅O₂⁺, 49.44); HPLC (1:5, hexane:diethyl ether, 2.1 min, 72%, 3.3 min, 28%); high resolution mass spectrum (EI) calcd for C₇H₁₁IO₃, M⁺ 269.9753, found 269.9762.

In order to assign stereochemistry to each diastereomer, the lactone mixtures were converted into the corresponding epoxides by methanolysis according to the following procedure. To a dried flask was added the lactone mixture (42.3 mg, 0.157 mmol), 3.0 mL of MeOH, and K₂CO₃ (21.7 mg, 0.157 mmol), and the resulting solution was stirred for 1 h, diluted with water, saturated with NaCl, extracted 3 times with diethyl ether, dried with MgSO₄, and concentrated in vacuo to yield a mixture

(23) Ph₃PCHCOCH₃ was prepared according to Ramirez and Dershowitz (Ramirez, F.; Dershowitz, S. *J. Org. Chem.* 1957, 22, 41).

of epoxides which were analyzed by capillary gas chromatography. Authentic methyl ester epoxy alcohols for comparison were prepared by using the erythro-selective vanadium-catalyzed Sharpless epoxidation procedure²⁴ on the methyl ester of **3** prepared by treatment of **3** with diazomethane.²⁵ Epoxy methyl esters from iodolactone mixture: ¹H NMR (250 MHz, CDCl₃) 3.94 (m, H-6), 3.70 (s, 3 H, OMe), 3.05 (dt, *J* = 5.9, 2.0 Hz, H-4), 2.81 (appt, *J* = 2.0 Hz, H-5), 2.48 (t, *J* = 7.2 Hz, 2 H, H-2), 1.91 (m, 2 H, H-3), 1.25 (d, *J* = 6.6 Hz, 3 H, H-7); minor isomer observed at 3.00, 2.78, 1.29; GC (5.5 min, 78%, 5.6 min, 22%); this mixture of epoxides closely resembled the Sharpless mixture by 250-MHz ¹H NMR and gave identical retention times and a very similar diastereomer ratio by capillary GC (5.5 min, 73%, 27%).²⁶ It thus follows that the major iodolactone is **4a** and the minor diastereomer is **4b**.

Acknowledgment. Partial support of this work in the form of an NSF grant to A.R.C. (CHE 8401197) is gratefully acknowledged. A helpful suggestion by Professor Collum (Cornell University) was incorporated into the introductory section.

Registry No. **3**, 105728-84-5; **3** methyl ester, 105762-40-1; **4a**, 105728-87-8; **4a** epoxy methyl ester, 105728-88-9; **4b**, 105814-95-7; **4b** epoxy methyl ester, 105834-46-6; Ph₃P=CHC(O)CH₃, 1439-36-7; OHC(CH₂)₂CO₂H, 692-29-5; 4-dioxolanebutanoic acid, 105728-85-6; 6-oxo-4-heptenoic acid, 105728-86-7.

(24) Sharpless, K. B. *Aldrichim. Acta* 1979, 12, 63.

(25) Diazomethane was prepared according to Moore and Reed (Moore, J. A.; Reed, D. E. *Organic Syntheses*; Wiley: New York, 1973; Collect. Vol. 5, p 351).

(26) It is not totally clear why these two epoxide regioisomers are formed preferentially. Methanolysis of the lactone ring must be faster than direct epoxide formation, since we observe neither the lactone epoxides derived directly from **4a** and **4b** nor their subsequent methanolysis/Payne rearrangement²⁷ epoxy alcohol products (neither of which correspond to the Sharpless diastereomers). There most likely is an iododiol ester intermediate in the methanolysis reaction that regioselectively forms the observed epoxide. We previously have observed similar selectivities in related 2-iodo 1,3-diols,^{3a} attributable to cis epoxides forming more slowly than trans.

(27) Payne, G. B. *J. Org. Chem.* 1962, 27, 3819.

(28) (a) Cha, J. K.; Christ, W. J.; Kishi, Y. *Tetrahedron Lett.* 1983, 24, 3943. (b) Cha, J. K.; Christ, W. J.; Kishi, Y. *Ibid.* 1983, 24, 3947. (c) Cha, J. K.; Christ, W. J.; Kishi, Y. *Tetrahedron* 1984, 40, 2247.

(29) For an interesting recent study of osmylation that supports a late transition state, see: Vedejs, E.; McClure, C. K. *J. Am. Chem. Soc.* 1986, 108, 1094.

(30) Schröder, M. *Chem. Rev.* 1980, 80, 187.

Estimation of Inner Shell Marcus Terms for Amino Nitrogen Compounds by Molecular Orbital Calculations

Stephen F. Nelsen,* Silas C. Blackstock, and Yaesil Kim

Contribution from the S. M. McElvain Laboratories of Organic Chemistry, Department of Chemistry, University of Wisconsin, Madison, Wisconsin 53706. Received June 4, 1986

Abstract: The rate constant k_{et} for electron transfer between the unsaturated bridgehead diazosesquibicyclo[2.2.2]octane (**1**) and **1**⁺(NO₃⁻) in CD₃CN was determined by proton NMR line broadening measurements to be $1.3 \times 10^4 \text{ M}^{-1} \text{ s}^{-1}$ at 23.5 °C, with activation parameters $\Delta H_{et}^{\ddagger} = 7.20 \text{ kcal/mol}$ and $\Delta S_{et}^{\ddagger} = -15.4 \text{ cal mol}^{-1} \text{ K}^{-1}$. k_{et} for its saturated analogue **2,2**⁺(NO₃⁻) is 7.0×10^2 (23.0 °C, CD₃CN), while that for **2**⁺(PF₆⁻), **2**²⁺(PF₆⁻)₂ is 2.1×10^4 (24.1 °C, CD₃CN), with activation parameters $\Delta H_{et}^{\ddagger} = 8.4 \text{ kcal/mol}$ and $\Delta S_{et}^{\ddagger} = -10.3 \text{ cal mol}^{-1} \text{ K}^{-1}$. Because k_{et} for *N,N,N',N'*-tetramethyl-*p*-phenylenediamine (**3**), **3**⁺(ClO₄⁻) in CH₃CN at 20 °C is 1.7×10^6 times that quoted above for **2,2**⁺, the inner shell Marcus term must dominate the *et* barrier for the hydrazine case. The Dewar group AM1 semiempirical MO calculation method successfully predicts this effect. These calculations also indicate that the inner shell term for **3** is far larger than previously accepted.

Lone pair-lone pair interactions cause tetraalkylhydrazines (R₄N₂) to undergo especially large geometry changes upon electron loss.¹ The nitrogens of neutral R₄N₂ are strongly pyramidal, and there is a rather weak electronic preference for the lone pairs to

be perpendicular (lone pair-lone pair dihedral angle $\theta = 90^\circ$). The cation radical R₄N₂⁺ has much flatter nitrogen atoms and a strong preference for coplanar lone pair axes ($\theta = 0$ and 180°). The unpaired electron is in the π^* orbital of the π -rich orbital hybrid predominately centered at the two nitrogen atoms, a situation described as a "three-electron π bond". Electron loss from R₄N₂ may be thought of as producing half a π bond between the nitrogens, which is the source of the large geometry change.

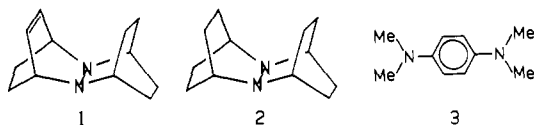
(1) (a) Nelsen, S. F. *Acc. Chem. Res.* 1981, 14, 131. (b) Nelsen, S. F. *Molecular Structures and Energetics*; Liebman, J. F., Greenburg, A., Eds.; VCH Publishers: Deerfield Beach, FL, 1986, Vol. 3, Chapter 1, p 1.

Table I. Comparison of Self-Exchange Electron Transfer Rate Constants for Bis-*N,N'*-sesquibicyclhydrazines **1** and **2** with Those of Tetramethyl-*p*-phenylenediamine (**3**) in Acetonitrile

compounds	temp (°C)	k_{et} (M ⁻¹ s ⁻¹)	k_{rel}	$\Delta G_{et}^{\ddagger a}$	$\Delta H_{et}^{\ddagger a}$	$\Delta S_{et}^{\ddagger b}$	ref
1,1 ⁺ (NO ₃ ⁻)	23.5	1.3×10^4	19	11.7 ₇	7.20 ^c	-15.8 ^c	<i>e</i>
2,2 ⁺ (NO ₃ ⁻)	23.0	7.0×10^3	1	13.4 ₂			<i>e</i>
2 ⁺ , 2 ⁺ (PF ₆ ⁻) ₂	24.1	2.1×10^4	30	11.5 ₁	8.47 ^d	-10.3 ^d	<i>e</i>
3,3 ⁺ (ClO ₄ ⁻)	20.0	1.17×10^9	1.7×10^6	4.98	2.63	-7.6	<i>f</i>
3 ⁺ , 3 ⁺ (ClO ₄ ⁻) ₂	20.0	6.7×10^7	9.6×10^4	6.65	4.97	-6.0	<i>f</i>

^akcal/mol. ^bcal mol⁻¹ K⁻¹. ^cAverage of two separate runs. Data appear in experimental section. ^dData appear in experimental section. ^eThis work. ^fReference 8.

Self electron transfer (et) between a neutral compound *n* and its cation radical *c*, a $\Delta G^\circ = 0$ process, occurs with a rate constant k_{et} above 10^8 M⁻¹ s⁻¹ for most organic compounds.² Electron exchange causes broadening of the ESR spectrum of *c* when *n* is added, which is frequently used to measure k_{et} . Not only do R₄N₂, R₄N₂⁺ mixtures not show ESR line broadening,³ most also do not show NMR line broadening for *n*, which is sensitive to slower k_{et} values. A method for preparing *N,N'*-bissesquibicyclic hydrazines which are forced into θ near 0° conformations was recently reported,⁴ and it was found that **1,1**⁺ mixtures show fast



enough electron exchange to give NMR line broadening, allowing accurate determination of k_{et} .⁵ We report here k_{et} values for both first and second electron exchanges (between *c* and the dication *d*) of the saturated analogue **2**, compare them with those for tetramethyl-*p*-phenylenediamine (**3**), and discuss the origin of the most striking differences in their behavior, the 1 000 000-fold difference in k_{et} for *n,c* exchange, and the faster *c,d* than *n,c* exchange for **2**, but slower *c,d* than *n,c* exchange for **3**.

Results: NMR Line Broadening Studies

1 proved to be an ideal substrate for accurate measurement of k_{et} by ¹H NMR line broadening. Both **1** and **1**⁺ salts can be isolated and purified, so solutions of known concentration can be prepared. The low values for k_{et} keep all the data collected well inside the slow exchange limit region, where the equation for broadening is surprisingly simple⁶ (eq 1). The exchange

$$\Delta\nu = (k_{et}/\pi)[c] \quad (1)$$

broadening $\Delta\nu$, the increase in line width at half-height for the NMR signal of *n* in the presence of *c*, depends only on the concentration of *c*. At faster exchange rates, as the fast exchange limit is approached, the broadening depends upon the ESR coupling constant in *c* for the hydrogen of *n* being observed. The fact that similar broadenings are observed for all hydrogens of **1**, despite a range of well over ten for their ESR splitting constants, is important evidence that the data are in the slow exchange limit. Slow exchange also requires that the peaks for *n* do not shift position as *c* is added, which was shown to be true for the approximately 30 min required for collection of data over a series of *c* concentrations. This is also a sensitive criterion for the absence of decomposition of *c*, because decomposition generates protons which exchange with *n*, shifting the peaks downfield. The vinyl hydrogen signal of **1** provides a well-resolved group of sharp lines which are easily simulated as the AA' portion of an AA'XX' pattern (XX' are the bridgehead hydrogens) with a line width of

0.8 Hz in CD₃CN, so that accurate broadenings may be determined by increasing the line width in a simulation until the experimental spectrum is matched. Solvent peaks were observed to remain unbroadened as **1**⁺ is added, demonstrating that radical concentrations did not become high enough to cause significant broadening in the absence of electron exchange. A final test of true slow exchange kinetic behavior as indicated by eq 1 is that addition of **2**⁺ to solution of **1** does not effect ν of **1** detectably, even at concentrations for which **1**⁺ causes over 50 Hz of broadening. **1,2**⁺ exchange has to be far slower, because **2** is 0.29 V (6.7 kcal/mol) easier to oxidize than **1**.

We were especially interested in obtaining data for **2**, which is unique among reported examples of R₄N₂ in giving isolation as well as cation radical salts, so that its second electron exchange can be studied as well as the first. Also, crystal structures are available for **2**, **2**⁺OTs⁻, and **2**⁺(PF₆⁻)₂,⁷ so that the amounts of the geometry change upon first and second electron removal are known. Unfortunately, **2** is not nearly as convenient for electron exchange broadening studies as is **1**. The only resolved ¹H NMR signal is that for the bridgehead hydrogens, which is a 5-Hz wide unresolved multiplet because of its extensive coupling to protons of three different chemical shifts, so that small broadenings are difficult to quantitate. We used a working curve of the accurately measured $\Delta\nu$ values for the vinyl signal of **1** vs. the observed line width of its bridgehead hydrogen, which is a good model for that of **2**, and saw enough broadening so that reasonable accuracy could be obtained. **2** is also significantly more oxidized to handle than is **1**, because it is much more rapidly air oxidized, but it is stable in the absence of oxygen. Most seriously, **2**⁺ is slowly decomposed by **2** on the timescale required for proton NMR measurements. Both a downfield shift of the NMR signals of **2** caused by the protons produced and a decrease in broadening caused by the disappearance of **2**⁺ are observed. The data were corrected for this decomposition by adding a correction to the $\Delta\nu$ recorded by using the observed 0.118₃ $\Delta\nu/\Delta\delta$ obtained from experiments in which **2,2**⁺ mixtures were allowed to stand. By using these corrected data, we obtained reasonably good fit to eq 1, although the correlation coefficient observed was 0.94 instead of the >0.99 obtained for **1,1**⁺. Fortunately, decomposition was not a problem for the *c,d* exchange of **2**, allowing determination of its activation parameters by varying the temperature. Data in acetonitrile obtained by NMR line broadening for these hydrazines are compared with the ESR line broadening data reported by Grampp and Jaenicke⁸ (GJ) for **3** in Table I.

Discussion

A. Comparison of Rates for **2 and **3**.** The data quoted for **3** are from the extensive study of five *p*-phenylenediamine derivatives in six solvents at various temperatures by GJ. They discuss a classical Marcus approach^{2,9} to the measured rate constants, by using the collisional theory eq 2, with $Z_0 T^{1/2} = 2 \times 10^{10}$ L mol⁻¹

$$k_{et} = Z_0 T^{1/2} \exp(-\Delta G^*/RT) \quad (2)$$

$$\Delta G^* = W^\ddagger + (\lambda_0 + \lambda_i)/4 \quad (3)$$

(2) Ebersson, L. *Adv. Phys. Org. Chem.* **1982**, *18*, 79.

(3) Nelsen, S. F.; Hintz, P. J.; Buschek, J. M.; Weissman, G. R. *J. Am. Chem. Soc.* **1975**, *97*, 4933.

(4) (a) Nelsen, S. F.; Blackstock, S. C.; Frigo, T. B. *J. Am. Chem. Soc.* **1984**, *106*, 3366. (b) Nelsen, S. F.; Blackstock, S. C.; Frigo, T. B. *Tetrahedron* **1986**, *42*, 1769.

(5) Nelsen, S. F.; Blackstock, S. C. *J. Am. Chem. Soc.* **1985**, *107*, 7189.

(6) (a) Bruce, C. R.; Norbert, R. E.; Weissman, S. I. *J. Chem. Phys.* **1956**, *24*, 473. (b) McConnell, H. M.; Weaver, H. E. *Ibid.* **1956**, *25*, 307. (c) McConnell, H. M.; Berger, S. B. *Ibid.* **1957**, *27*, 230.

(7) Nelsen, S. F.; Blackstock, S. C.; Haller, K. J. *Tetrahedron*, in press.

(8) (a) Grampp, G.; Jaenicke, W. *Ber. Bunsenges. Phys. Chem.* **1984**, *88*, 325. (b) Grampp, G.; Jaenicke, W. *Ibid.* **1984**, *88*, 335. (c) Grampp, G.; Jaenicke, W. *J. Chem. Soc., Faraday Trans. 2*, **1985**, *81*, 1035.

(9) (a) Marcus, R. A. *Annu. Rev. Phys. Chem.* **1964**, *15*, 155. (b) Marcus, R. A. *Special Topics in Electrochemistry*; Rock, P. A., Ed.; Elsevier: Amsterdam, 1977; p 161.

$s^{-1} K^{-1}$, and the usual breakdown of ΔG^* into inner and outer shell terms as indicated in eq 3. This makes $\Delta G^* = 3.33$ kcal/mol,¹⁰ which we note removes one third of the transition state theory ΔG^* (Table I), although ΔG^* and ΔG^\ddagger are often considered to be more or less interchangeable in concept. The work term W^p is zero for an n,c self-exchange, and the usual Born solvent continuum model was used to estimate the outer shell (solvent reorganization) term, eq 4, (the constant given for distances in Å).

$$\lambda_0 = 332.4g(r,d)\gamma, \text{ kcal/mol} \quad (4)$$

γ is a solvent polarity parameter, $\gamma = (1/n^2 - 1/\epsilon)$, with n the refractive index and ϵ the dielectric constant, numerically 0.527 for acetonitrile at 20 °C. $g(r,d)$ is a distance parameter, which is usually used in the spheres approximation given in eq 5. Note

$$g(r,d), \text{spheres} = (1/2r_1 + 1/2r_2 - 1/d) \quad (5)$$

that eq 5 gives $g(r,d) = 1/2r$ for self-transfer if the spheres touch at the transition state so $d = 2r$. GJ obtained an "experimental" value of $g(r,d) = 0.049 \text{ \AA}^{-1}$ from the plot of $\ln k_{et}$ vs. γ by using eq 3 and 4, which corresponds to $r = 10.2 \text{ \AA}$ in the spheres approximation of eq 5. This is much larger than the radius of 3, but GJ pointed out that 3 is far from being spherical, and they do a sophisticated evaluation of $g(r,d)$ for ellipsoids to replace eq 5. By using the crystallographic ring centers distance of 5.46 \AA for the et transition state, the ellipsoid calculation gave $g(r,d) = 0.0537 \text{ \AA}^{-1}$ (corresponding to $r = 9.3 \text{ \AA}$ in the spheres approximation), and they conclude that assuming 3 to be a sphere leads to a large error.¹¹ Instead of ignoring λ_i , as is typically done for organic molecules, they evaluated it with a Hale-type analysis by using Hückel-derived bond orders^{8a} to obtain $\lambda_i(\text{theor}) = 3.6$ kcal/mol,¹² which they note is larger than obtained for hydrocarbons in a similar manner. Evaluations using PPP calculations gave $\lambda_i(\text{theor}) = 7.8$ kcal/mol, and an estimation using the X-ray data gave 11.3 kcal/mol.^{8c} An "experimental" λ_i value was estimated from the intercept of the k_{et}, γ plot to be 8.4 ± 0.7 kcal/mol, assuming that $g(r,d) = 0.0491$. When they actually break ΔG^* down into inner and outer shell components, however, they choose the smaller calculated number, giving $\Delta G^*(\text{calcd})$ of 2.56 kcal/mol (77% of the observed value) partitioned as 82% $\Delta G^*_0 = \lambda_0/4 = 2.1$, 18% $\Delta G^*_i = 0.4$. In the later paper,^{8c} it is argued that tunneling effects are important, and an effective ΔG^*_i at 293 K from the largest (X-ray) λ_i estimate is only 1.4 kcal/mol. For the second electron transfer, c,d of 3, GJ obtain $\lambda_i(\text{theor})$ by HMO of 3.4 kcal/mol, close to that for the first transfer, and conclude that the 17-fold drop observed in k_{et} must arise from the work term

$$W^p = 664.8/\epsilon d, \text{ kcal mol}^{-1} (d \text{ in } \text{\AA}) \quad (6)$$

which they evaluate from eq 6 to be 2.07 kcal/mol at a distance of 8.54 Å, and 3.13 kcal/mol at a distance of 8.54 Å, and 3.13e ring centers in crystalline 3⁺, which are close to the observed 2.34 kcal/mol ΔH^\ddagger difference. In their second paper GJ note^{8b} that while the temperature dependence of k_{et} using the Marcus analysis is not quite correct, everything can be brought into agreement by assuming a fairly small temperature dependence of the distance between the centers at the transition state and point out that on the whole, Marcus theory rather well with their extensive experimental data. In the later paper^{8c} it is argued that cation, ClO₄⁻ and cation, neutral interactions must be allowed for, if the temperature dependence is to be fit to Marcus theory.

The sesquibicyclic hydrazines 1 and 2 are qualitatively similar in size to 3 (they are C₁₂N₂ compounds while 3 is C₁₀N₂), so we

(10) The 12.9 kJ/mol ΔG^* given in ref 8a, Table VI column 9, entry R_{IV}/S_{IV} is apparently a misprint for 13.9.

(11) (a) The difference in the semiaxes employed must be important in obtaining smaller $g(r,d)$ values in the ellipsoid correction to the spheres approximation. It is surprising to use that 1.55 Å was chosen as the shortest semiaxis for 3⁺ because the interring distance quoted in the X-ray paper said to be the interring distance is 3.55 Å, which is twice 1.78. (b) Also, see: ref 2, 115–121.

(12) We thank Professor Grampp for pointing out to us that the papers of ref 8 were in error by a factor of 2 in calculation λ_i (two molecules are involved at the transition state). The numbers quoted here are the proper ones.

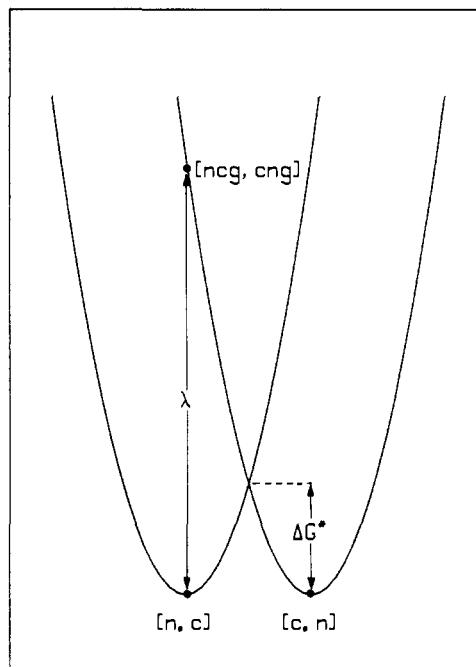


Figure 1. Diagram showing the relationship between vertical electron transfer and the barrier for thermal electron transfer.

would expect their outer shell solvent reorganization terms λ_0 to be quite similar. The much lower rate constants for 1 and 2 than for 3 (see the k_{et} column of Table I) can only reasonably be attributed to much larger inner shell terms for the hydrazines. λ_i dominance is also indicated by the 30-fold rate increase for the d,c electron transfer for 2 compared to the n,c transfer. The work terms ought to be similar for the d,c transfers of 2 and 3 (although the distance for electron transfer at the transition state, in these as in all other intermolecular cases, is unknown), and the work term leads to a 17-fold decrease in rate for 3. It is known from the X-ray structures that the geometry change between 2²⁺ and 2⁺ is substantially smaller than that between 2⁺ and 2. The size of λ_i must clearly be addressed to understand the rate changes between 2 and 3, and the sum of vibrational force constant type of analysis used by GJ for 2 would be cumbersome at best. Furthermore, 2 has only a two atom π system, but the charge is extensively delocalized onto the alkyl groups, and trying to use Hückel or PPP calculations here would clearly be fruitless. Furthermore, a real problem with force-constant analyses for 2 is that the most important changes occur in low-frequency bending motions, which do not even occur in the IR region for 2⁺.

B. MO Treatment of Inner Shell Relaxation. The complexity of these molecules prohibits using high-level ab initio methods to calculate their properties. We were previously discouraged from attempting to use semiempirical methods by their failure to be able to handle nitrogen inversion in any reasonable way. For example, MNDO gets trimethylamine to be flat at nitrogen, which is disastrous for this problem, where the most important geometry change involved is flattening at nitrogen. Dewar's latest semiempirical method,¹³ AM1, has successfully decreased the too large 1,3-nonbonded interactions which have plagued previous methods and proves to be surprisingly good at reproducing the amount of bend in all three oxidation states of R₄N₂, encouraging us to try to use it to calculate λ_i values. The relationship between the relaxation energies of n and c and the Marcus γ value may be considered by use of the diagram typically employed in Marcus treatments for noninteracting self electron transfer (et) shown in Figure 1. The two parabolas represent energy wells for pairs of n and c, before and after et. The vertical distance from one minimum to the other parabola, labeled λ , is the energy difference

(13) Dewar, M. J. S.; Zoebisch, E. G.; Healy, E. F.; Stewart, J. P. *J. Am. Chem. Soc.* 1985, 107, 3902. We thank Dr. Stewart for a copy of program MOPAC 2.14 and later 3.00, which were used for the calculations.

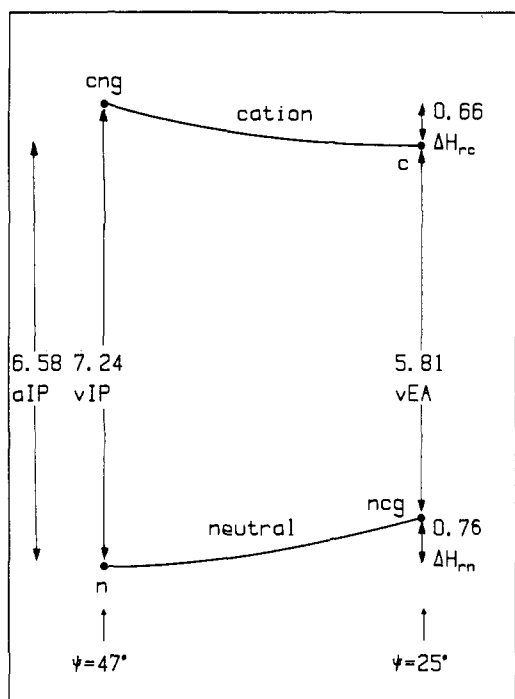


Figure 2. AM1 calculated energies of n, c, ncg, and cng for **2**. The numbers are differences in heats of formation in eV.

between the equilibrated pair and the vertical et pair having the neutral species at the geometry of the cation (ncg) and the cation at the geometry of the neutral species (cng). The enthalpy portion of the Marcus λ value is, therefore, simply the sum of the relaxation energy between the vertical cation and the relaxed cation ($\Delta H_{rc} = \Delta H(\text{cng}) - \Delta H(\text{c})$) and that for the neutral compound ($\Delta H_{rn} = \Delta H(\text{ncg}) - \Delta H(\text{n})$). Although the Marcus treatment is always supposed to represent ΔG and not ΔH , the calculations we have seen for λ , are really only for ΔH anyway, although this is often not pointed out explicitly. For most organic cases it has been considered that the parabolas represent almost exclusively outer shell, solvent energy changes, but they also include inner shell, compound reorganization terms, and in a calculation not including solvent must just represent λ . The point at which the parabolas cross is $\Delta G^* = \lambda/4$ above the minimum energy and is the source of the factor of 4 in eq 3; it represents the thermal barrier to electron transfer. For bimetallic intervalence complexes, it is now common¹⁴ to determine λ from the optical absorption spectrum and report ΔG^* values by dividing the energy by 4. Figure 1 introduces an artificial symmetry into the electron transfer process, however. Because n and c have different geometries, ncg and cng will in general occur at different energies above n and c, respectively, and an advantage of an MO approach to determining the individual relaxation energies is that one can consider whether significant deviations from the factor of 4 are predicted to occur, which appears not to be a question if Figure 1 is used.

Figure 2 shows the results of AM1 calculations for **2**, showing n and c as well as their vertically related species, ncg and cng. The horizontal axis represents the geometry change between relaxed n and c geometries, which is particularly easy to think about for **2** because the change in the flap angle Ψ will be shown



to be the dominant, though not the exclusive factor. ΔH_{rc} is in principle experimentally measurable as the difference between the vertical ionization potential, vIP, obtained from photoelectron

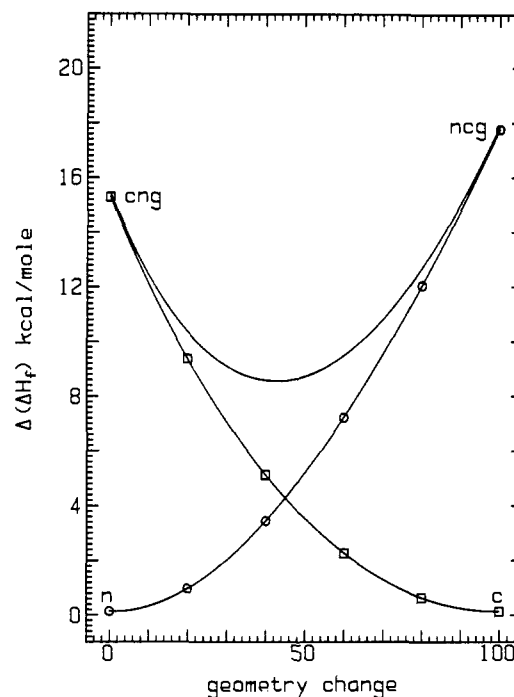
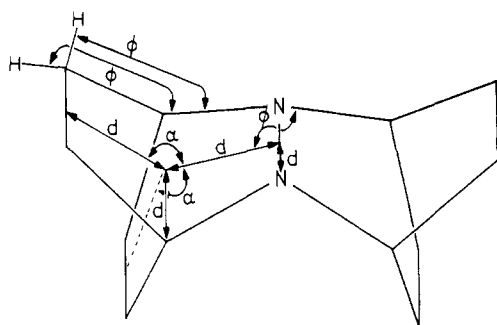


Figure 3. Plots of change in the AM1 calculated heat of formation for neutral **2** and its cation radical as the geometries are changed from that of the neutral (0) on the geometry change coordinate to that of the cation radical (100).

spectroscopy, and the adiabatic ionization potential, aIP, which has recently become available for several R_4N_2 examples by high-pressure mass spectrometry measurements.¹⁵ We are not aware of a good experimental way to measure ΔH_{rn} , but have labeled the n, cng gap as the vertical electron affinity, vEA. AM1 does a good job of getting the amounts of bend at nitrogen for **2**, obtaining $\Psi = 46.6^\circ$ for n (the X-ray value is 47.8°) and 25.0° for c (the X-ray value is 27.4°),⁷ although the X-ray of 2^+ is of rather low quality; agreement is closer for 1^+ , where the X-ray is of better quality). Neutral **2** has the lone pair–lone pair dihedral angle $\theta = 15^\circ$ by X-ray, but we were unable to find a significantly twisted structure of lower energy than the eclipsed $\theta = 0^\circ$ structure used in this work by AM1 and have, therefore, used D_{2d} symmetry for all three oxidation states, which greatly simplifies the calculations. Distances, angles, and dihedral angles (25) are necessary to describe **2** even using all of the symmetry possible, and all were optimized in these calculations. The asymmetry mentioned above is indeed calculated to be present, and ΔH_{rc} is calculated to be 2.4 kcal/mol (14%) lower than ΔH_{rn} . This makes the Franck–Condon transition state for electron transfer not occur exactly at 50% on the geometry change coordinate but at 45%, as illustrated in Figure 3, where n and c are placed at $\Delta \Delta H^\circ = 0$, so the point of crossover can be easily located. The intermediate geometry points were obtained in the following way. Of the 25 parameters 16 hardly change at all between n and c, and it is acceptable to use their average values at all geometries; doing this only raises the calculated energies of n, c, ncg, and cng by a negligible 0.14, 0.13, 0.15, and 0.09 kcal/mol, respectively. The remaining nine quantities (indicated on the drawing below; ϕ indicates dihedral angles, α , bond angles, and d , distances) were stepped in 20% increments between their values for n and for c, and the energies thus calculated were connected by interpolating smooth curves. Ψ dominates the calculated changes, as was shown by separate calculations in which Ψ was fixed, and everything else was optimized, resulting in the estimates that 70% of the cng,n energy gap and 73% of the ncg,c energy gap is obtained just by fixing Ψ . Also plotted in Figure 3 is the sum of the distortion energies,

(14) (a) Taube, H. *Ann. N. Y. Acad. Sci.* **1978**, 481. (b) Meyer, T. J. *Ann. N. Y. Acad. Sci.* **1978**, 496. (c) Meyer, T. J. *Acc. Chem. Res.* **1978**, 11, 94. (d) Hush, N. S. *Prog. Inorg. Chem.* **1967**, 8, 39.

(15) (a) Meot-Ner (Mautner), M.; Nelsen, S. F.; Willi, M. F.; Frigo, T. *B. J. Am. Chem. Soc.* **1984**, 106, 7384. (b) Nelsen, S. F.; Rumack, D. T.; Meot-Ner (Mautner), M. *J. Am. Chem. Soc.*, in press.



which corresponds to the ΔH barrier for electron transfer at each point. The dissymmetry removes the requirement that the minimum distortion energy sum come at the curve crossing point, but it does not come far from it, as a minimum of 8.55 kcal/mol was obtained at 42% on the geometry change coordinate, while the sum is 8.56 kcal/mol at the curve crossing at 45%. The value of $\lambda_i(\text{AM1})$ is 32.84 kcal/mol, so the stepping calculations give an AM1 energy surface enthalpy barrier of 26% of λ_i instead of the 25% predicted by assuming parabolas crossing, not a significant difference. Figure 4 is exactly analogous, for the c,d electron transfer. The relaxation energies are calculated to be significantly smaller than for the first electron transfer, as expected because the geometry changes are smaller. The dissymmetry is greater, ΔH_{rc} being 4.5 kcal/mol (47%) smaller than the stiffer ΔH_{rd} , and crossover occurs at 56%, where ΔH^*_i (AM1) is 28% of $\lambda_i(\text{AM1})$; a lot of dissymmetry is clearly required for very significant deviations between the Franck-Condon transition-state energy and that of $\lambda_i/4$.

An extreme case of ΔH_{rc} , ΔH_{rn} dissymmetry is obtained for electron transfer between trimethylamine and its cation radical, as shown in exactly the same fashion in Figure 5. Here n is calculated to be so much easier to bend than is c that the energy sum continuously increases as the transition state is distorted from c toward n. The curves cross at 51% on the geometry change coordinate where the curve sum is 29.5% of λ_i . Because all points on the curve sum plot correspond to Franck-Condon transition states for electron transfer, AM1 predicts a huge geometry difference between the minimum ΔH transition state and the curve crossing point, although the energy difference is small. It is interesting to note that n,c et in saturated amines is almost certainly not, however, a noninteracting case as has been assumed in constructing Figure 5. In exactly the same sense as removal of an electron from R_4N_2 makes half a π bond between the nitrogens, removal of an electron from medium ring bridgehead diazabicyclic amines (R_6N_2) generates half a σ bond between the nitrogens, as has been demonstrated by Alder and co-workers.¹⁶ Even larger geometry changes among n, c, and d than occur for hydrazines have been demonstrated by X-ray crystallography for 1,6-diazabicyclo[4.4.4]tetradecane,^{16b} and electron transfers are astonishingly slow; the highly exothermic n,d electron transfer was found to have k_{et} of $0.2 \text{ M}^{-1} \text{ s}^{-1}$ in acetonitrile.¹⁷ Although higher level calculations¹⁸ as well as semiempirical ones predict the $3e-\sigma$ bond for H_3N, NH_3^+ , AM1 does not obtain such a species as an energy minimum for Me_3N, Me_3N^+ . Experimentally, electron transfer would not be expected to occur, because hydrogen atom transfer would be much more rapid.¹⁹

Interaction between the units undergoing et by three-electron σ bonding such as occurs in medium ring bicyclic diamines is neither predicted theoretically nor seen experimentally for bis-hydrazines which have the two hydrazine units held close in space,²⁰ and 1 and 2 as well as 3 should be cases of noninteracting

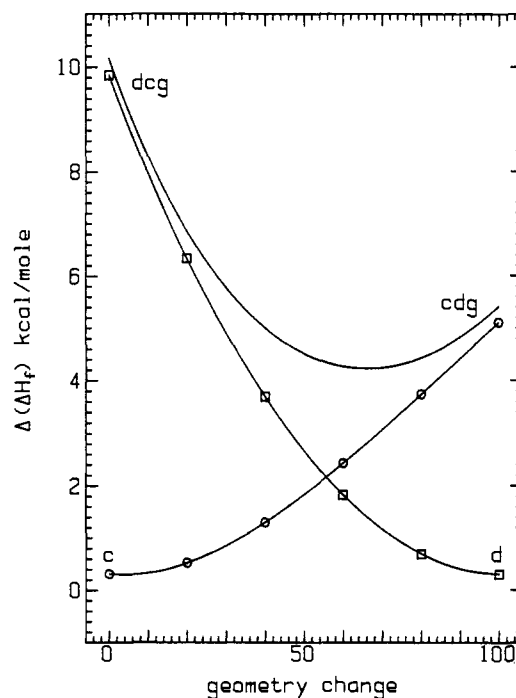


Figure 4. As Figure 3, for 2^+ and 2^{2+} . 0 on the geometry change coordinate represents the cation geometry and 100 that of the dication.

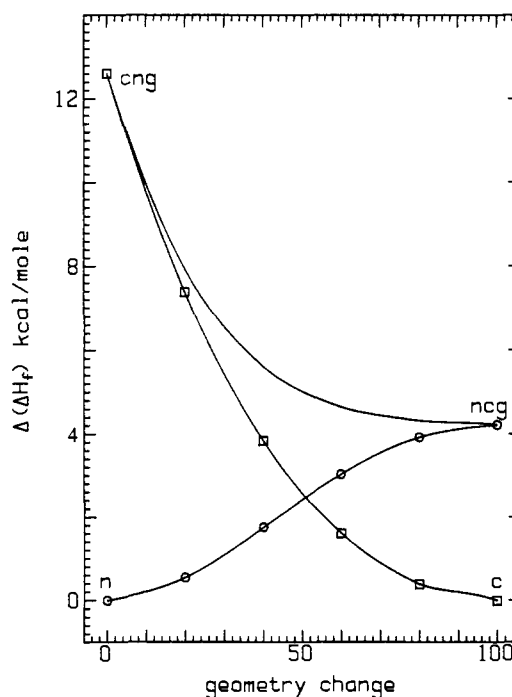


Figure 5. As Figure 3, for trimethylamine and its cation radical.

Table II. AM1 Calculated Relaxation Energies

et pair	ΔH_{rc}^a	ΔH_{rn}^a	ΔH_i^{*a}	obsd $\Delta H_{ei}^{*a,b}$
$2,2^+$	17.63	15.22	8.21	
$2^+,2^{2+}$	5.12	9.67	3.70	8.5
$3,3^+$	4.21	4.01	2.06	2.63
$3^+,3^{2+}$	4.67	4.51	2.30	4.97

^akcal mol⁻¹. ^bFrom Table I.

(16) (a) Alder, R. W.; Sessions, R. B. *Chemistry of Azo, Nitroso, and Nitro Compounds and Their Derivatives*; Patai, S., Ed.; Wiley: New York, 1982; Chapter 18, p 762. (b) Alder, R. W.; Orpen, A. G.; Sessions, R. B. *J. Am. Chem. Soc.*, **Chem. Commun.** **1985**, 949.

(17) Alder, R. W.; Sessions, R. B. *J. Am. Chem. Soc.* **1979**, *101*, 3651.

(18) Bouma, W. J.; Radom, L. *J. Am. Chem. Soc.* **1985**, *107*, 345.

(19) Nelsen, S. F.; Ippoliti, J. T. *J. Am. Chem. Soc.* **1986**, *108*, 4879.

(20) Nelsen, S. F.; Willi, M. R.; Mellor, J. M.; Smith, N. M. *J. Org. Chem.* **1986**, *51*, 2081.

electron transfer to which the Marcus development of Figures 1 and 2 applies. Table II shows AM1 the relaxation energies plotted in Figures 3 and 4 for 2 as well as exactly analogous calculated values for 3. We note that the AM1 ΔH_i^* values predict the observed faster second electron transfer for 2 but slower electron transfer for 3 nicely and also give good reason for the

1 000 000-fold slower first electron transfer for **2** than for **3**. The ΔH^{\ddagger}_i value obtained cannot be off very significantly for the first electron transfer of **2**, which must surely have a barrier dominated by λ_i . Experimental data for ΔH_{rc} values of hydrazines will be published elsewhere, but it is already clear that the AM1 calculated values do not differ from the experimental ones by more than 10% for several cases and are often smaller than the measured values for hydrazines with θ far from 90°. As pointed out above, there is a close relationship between ΔH_{rc} and ΔH^{\ddagger}_i . Even if the values happened to be about right for hydrazines, maybe they are still very poor for amines. Unfortunately there is no experimental data available for ΔH_{rc} of aromatic amines, but some does exist for other amines (estimated from photoelectron spectroscopy measurements), and AM1 does not do a bad job of predicting them. For example Aue and co-workers²¹ quote ΔH_{rc} of 15.9 kcal mol⁻¹ for NH₃, while AM1 gets 15.63 and that for trimethylamine is quoted at 17.7 kcal/mol, while AM1 gets 12.60. For the bridgehead diamine 1,4-diazabicyclo[2.2.2]octane, where the photoelectron spectrum is especially favorable for measuring aIP as well as vIP, Heilbronner and co-workers²² obtained $\Delta H_{rc} = 7.46$, while AM1 obtains 7.71 kcal/mol. There is certainly no evidence from these comparisons that AM1 seriously overestimates relaxation energies for amino nitrogen compounds. The 2.06 kcal/mol AM1 value for ΔH^{\ddagger}_i of **3** should be compared with corrected¹² values of 0.9 (Hückel), 2.0 (PPP), and 2.8 (X-ray) kcal/mol from Grampp's work.⁸

Although it is well-known that λ_i is large for many inorganic self et reactions,²³ it has unusually been assumed that et kinetics for most organic systems are dominated by λ_0 .²⁴ In their most recent paper,^{8c} GJ avoid drawing the opposite conclusion by suggesting that tunnelling is important. Although the entropy term ΔS^{\ddagger}_{et} is somewhat more negative for **1,1**⁺ than it is for **3,3**⁺, the ΔH^{\ddagger} term accounts for most of the observed rate ratio (from the data of Table I, at 20 °C, the 1.04×10^5 rate constant ratio can be partitioned as a factor of 2 600 for the ΔH^{\ddagger} term and 40 for the ΔS^{\ddagger} term). Variation in a preexponential term, such as including an electronic transmission coefficient k_{et} (omitted from the simple treatment of eq 2), appears in the entropy. The observed enthalpy of activation is not very far from that obtained by what we (and JG) argue is a reasonable estimate of ΔH^{\ddagger}_i for **3,3**⁺, and the slowing of the rate when ΔH^{\ddagger}_i gets larger in going to the sesquibicyclic systems is also about what is expected from a large λ_i term. We suggest that the assumption that organic et kinetics are dominated by λ_0 has largely been based on the fact that the Born approach of eq 4 calculates ΔG^*_0 values which are as large as experiment (unless the molecules do not have to touch to get electron transfer, which has not seemed likely to many people), so no room was left for a ΔG^*_i term. It is certainly true that the λ dependence predicted by eq 4 is observed for **3**⁸ and a host of other compounds with k_{et} above 10^8 M⁻¹ s⁻¹, but linear $\ln(k_{et})$ vs. γ plots certainly do not occur for **2**,⁵ so one probably should not assume no γ dependence for λ_i as GJ did in their analysis.⁸ Something is affecting k_{et} as solvent is changed to buck

out the "normal" γ dependence for **2**, and dependence on viscosity has been both predicted and seen for high λ_i cases.²⁵ We will not discuss solvent dependence of k_{et} further here, but considerably more obviously needs to be said in the future.

We suggest that a reasonable conclusion from this work is that there is now serious question as to whether **3** electron transfers are as greatly dominated by ΔG^*_0 as assumed from the classical Marcus treatment⁸ and that if this is true, errors in the size of λ_0 as given by eq 4 might be larger than previously thought.

Experimental Section

Compound preparation details are given elsewhere.^{4,7}

A typical procedure for data acquisition for line broadening studies follows. Neutral **1** (29.2 mg) was dissolved in 600 μ L of CD₃CN which had been passed through a plug of activated neutral alumina and deaerated with a steam of nitrogen for 20–30 minutes, a 500- μ L aliquot transferred via syringe to a deaerated 5-mm NMR tube equipped with a septum, and the spectrum of neutral recorded on a Bruker 270-MHz NMR spectrometer. Aliquots of a similarly prepared solution of 3.56 mg of **1**⁺NO₃⁻ in 300 μ L of deaerated CD₃CN were transferred via syringe to the neutral sample, the tube was shaken vigorously, and the FID was recorded. Aliquots of 15, 20, 30, 30, 30, and 30 μ L were added in succession, and the probe temperature was measured before and after the run by using a Doris Model 400A Trendicator thermocouple. All FID data were stored on 8-in. DS/DD floppy discs, allowing data acquisition to take 22 min for the entire series. No change in line width or peak position was found after waiting 30 min after the last aliquot addition. The exchange broadenings were determined by the increase in line width necessary to simulate the vinyl region of each spectrum by using program WEASEL.²⁶ For **2**⁺,**2** exchange, exchange broadenings were determined from a working curve of observed bridgehead hydrogen half-width vs. simulated vinyl hydrogen exchange broadening for **1**.^{27a} The broadening, concentration data and plots from which the numbers in Table I were derived appear in the thesis of S. C. Blackstock.^{27b}

The variable temperature studies were carried out varying the temperature of samples of n.c. or c.d.

Run 1 of **1,1**⁺NO₃⁻: Sample 5.0₄ mM in **1**⁺, 126.6 mM in **1** in CD₃CN. Exchange broadening, Hz [temperature, °C]: 19.0 [21.7], 11.0 [11.5], 6.5 [0.6], 3.6 [-10.5] gave $\Delta H^{\ddagger} = 7.2_6$ kcal/mol, $\Delta S^{\ddagger} = -15.3$ cal/deg mol, ΔG^{\ddagger} (21.7 °C) 11.7₈ kcal/mol. Run 2: sample 4.9₂ mM in **1**⁺, 172.6 mM in **1** in CD₃CN. Exchange broadening, Hz [temperature, °C]: 14.2 [+21.5], 7.7 [+9.8], 2.4 [-12.9], 1.7 [-19.4], 9.0 [+10.3] gave $\Delta H^{\ddagger} = 7.1_3$ kcal/mol, $\Delta S^{\ddagger} = -16.3$ cal/deg mol, ΔG^{\ddagger} (21.5) 11.9₂.

Solution 8.9 mM in **2**⁺(PF₆)₂ and 100.7 mM in **2**⁺(PF₆)⁻ in CD₃CN. Exchange broadening, Hz [temperature °C]: 61.4 [25.3], 37.0 [13.9], 27.8 [7.6], 20.8 [1.6], 15.8 [-3.7], -11.2 [-10.4], activation parameters quoted in Table I.

Acknowledgment. We thank Professor Grampp for useful discussions of electron transfer theory. We thank the National Science Foundation and the National Institutes of Health for partial financial support of this work under Grants CHE-8415077 and GM-29549.

Registry No. **1**, 105616-08-8; **2**, 90046-49-4; **3**, 100-22-1.

(25) (a) Harrer, W.; Grampp, G.; Jaenicke, W. *Chem. Phys. Lett.* **1984**, *112*, 263. (b) Kuznetsov, A. M. *Soviet Electrochem.* **1984**, *20*, 1226. (c) Ovchinnikova, M. Ya. *Russ. Theor. Exper. Chem.* **1981**, *17*, 507. (d) Genett, Th.; Milner, O. F.; Weaver, M. J. *J. Phys. Chem.* **1985**, *89*, 2787. (e) Hupp, J. T.; Weaver, M. J. *Ibid.* **1984**, *88*, 1463. (f) calef, D. F.; Wolynes, P. G. *Ibid.* **1983**, *87*, 3387. (f) Newton, M. D.; Sutin, N. *Annu. Rev. Phys. Chem.* **1984**, *35*, 457. (g) Sutin, N. *Prog. Inorg. Chem.* **1983**, *30*, 442.

(26) Written by P. F. Schatz, University of Wisconsin.

(27) (a) The curve is linear with a slope of 1 above about 20 Hz and curves to 6-Hz bridgehead with 0-Hz exchange broadening. The data are plotted in the following: Blackstock, S. C. Thesis, University of Wisconsin, 1985, p 160. (b) Blackstock, S. C. Thesis, University of Wisconsin, 1985, pp 203–207.

(21) Aue, D. H.; Webb, H. M.; Bowers, M. T. *J. Am. Chem. Soc.* **1976**, *98*, 311.

(22) Alder, R. W.; Arrowsmith, R. J.; Casson, A.; Sessions, R. B.; Heilbronner, E.; Kovac, B.; Huber, H.; Taagepera, M. *J. Am. Chem. Soc.* **1981**, *103*, 6137.

(23) See, for example, Sutin, N. *Prog. Inorg. Chem.* **1983**, *30*, 1441 and ref 2, p 114.

(24) Reference 2, pp 113–114.